GEOPHYSICAL RESEARCH LETTERS, VOL. 37, L09804, doi:10.1029/2010GL042904, 2010



# Use of A-Train data to estimate convective buoyancy and entrainment rate

Zhengzhao Johnny Luo,[1] G. Y. Liu,[1] and Graeme L. Stephens[2]

Received 12 February 2010; accepted 31 March 2010; published 6 May 2010.

[1] This study describes a satellite-based method to estimate simultaneously convective buoyancy (B) and entrainment rate ($\lambda$). The measurement requirements are cloud-top height (CTH), cloud-top temperature (CTT), cloud profiling information (from radar and lidar), and ambient sounding. Initial results of the new method applied to A-Train data are presented. It is observed that tropical oceanic convection above the boundary layer fall into two groups: deep convection (DC) and cumulus congestus (Cg). DC tend to have negative buoyancy near cloud top and $\lambda <$ 10%/km. Cg are further divided into two groups due to the snapshot view of the A-Train: one has positive buoyancy and $\lambda \leq$ 10%/km and the other has negative buoyancy and $\lambda$ reaching up to 50%/km. Uncertainty analysis is conducted showing that CTT and CTH are the primary source of errors, but they do not affect our conclusions qualitatively. Brief comparisons with previous studies indicate the results of this study are broadly consistent with these earlier studies. Although most of the initial results are expected, this study represents the first time, to our knowledge, that satellite data are used to estimate convective buoyancy and entrainment rate. This new, space-borne method presents an opportunity for a number of follow-up investigations. For example, it serves as a bridge to connect A-Train observations (and follow-up missions) to GCM cumulus parameterizations. **Citation:** Luo, Z. J., G. Y. Liu, and G. L. Stephens (2010), Use of A-Train data to estimate convective buoyancy and entrainment rate, *Geophys. Res. Lett.*, *37*, L09804, doi:10.1029/2010GL042904.

## 1. Introduction

[2] Traditionally, convective processes such as buoyancy and entrainment are studied most often using data collected during field campaigns [e.g., *Heymsfield et al.*, 1978] or from cloud-resolving model simulations [e.g., *Lin and Arakawa*, 1997]. Not much attention has been paid to satellite observations probably because they are not considered as offering detailed views of convective-scale processes. With the launch of new generation instruments, most notably the TRMM (Tropical Rainfall Measuring Mission) and CloudSat radars, however, we are now able to view convection from a fundamentally new standpoint, and by relating these new dimensions of Earth observations to existing satellite capability, we are entering into a stage where innovative analysis of satellite data reveal tremendous new insights into convective processes. The purpose of this paper is to introduce a satellite-based method to estimate convective buoyancy and entrainment rate through synergistic use of A-Train data (see *Stephens et al.* [2002] for an overview of A-Train) and to discuss its potential applications.

[3] Several recent studies by *Luo et al.* [2008a, 2008b, 2009] analyzed tropical convection and hurricanes observed by CloudSat and other A-Train instruments. It has been shown that the synergistic use of the cloud profiling radar (CPR) and infrared (IR) radiometer is particularly useful in revealing new information about the underlying convective processes. For example, simultaneous measurements of cloud-top temperature, cloud-top height and cloud internal vertical structure allow us to deduce the stages in lifecycle of penetrative deep convection: incipient penetrating convection has colder top (despite lower height) and large radar echoes being transported to greater altitude, whereas dissipating deep convection exhibits warmer top (despite greater height) and radar echoes falling back to lower altitude [*Luo et al.*, 2008b]. Since A-Train (and most other polar orbiting satellites) view convection as passing snapshots (i.e., they do not capture the time evolution of the fast-evolving clouds), knowledge of convective life stage becomes important in that it gives the "static" snapshots some "dynamic" context.

[4] Following this line of research, we develop a new method that can be used to estimate convective buoyancy and entrainment rate from A-Train data. Convective buoyancy is closely related to convective lifecycle: incipient convection is usually positively buoyant, while overshooting and decaying convection tend to be negatively buoyant. Entrainment rate describes how effectively environmental air enters into clouds and dilutes the in-cloud air. Convective entrainment affects buoyancy and is critical in determining the final fate of convection: a highly diluted convective plume is likely to lose buoyancy at an intermediate level, thus becoming cumulus congestus; a relatively undiluted convection, on the other hand, will be able to ascend to great altitude. Some may even penetrate into the lower stratosphere.

[5] The layout of the paper is as follows: Section 2 gives a detailed account of the methodology, as well as data used. In section 3, initial results of the new method applied to A-Train data in the tropics are presented and discussed in light of our understanding of tropical convection. Section 4 analyzes uncertainties associated with the method and compares the initial results with previous studies. Section 5 summarizes the paper and discusses potential applications.

## 2. Data and Methodology

[6] Buoyancy (B) can be expressed as: $B = g[\frac{T' - T}{T} + 0.61 (q'_v - q_v) - q'_c]$,where T′, $q'_v$, and $q'_c$ refer to, respectively,

[1]Department of Earth and Atmospheric Sciences and NOAA-CREST Center, City College of New York, New York, New York, USA.
[2]Department of Atmospheric Science, Colorado State University, Fort Collins, Colorado, USA.


0094-8276/10/2010GL042904

temperature, specific humidity and hydrometeor mixing ratio inside clouds. T and $q_v$ are the corresponding quantities for the ambient environment. The three terms in the squared bracket represent the contributions to buoyancy from 1) temperature variation, 2) water vapor variation, and 3) hydrometeor loading, respectively. From a satellite perspective, only B near cloud top can be estimated because the temperature profile inside the cloud is not available. We use $T' - T$ to illustrate how this is done: IR brightness temperature ($T_b$), when corrected for limited cloud-top emissivity (discussed in next paragraph), can be interpreted as cloud-top temperature (CTT) or T′. But this information alone is not enough because without knowing independently the cloud-top height (CTH), we cannot make use of the ambient sounding to decide the corresponding T of the environment *for the same height level*. The minimum observational requirements are independent, simultaneous measurements of CTT and CTH, as well as ambient sounding. CloudSat and MODIS (Moderate-Resolution Imaging Spectroradiometer) onboard Aqua, which fly in formation with each other being separated by only ~2 min, make an ideal observational package for this purpose. CALIPSO (Cloud-Aerosol Lidar and Infrared Pathfinder Satellite Observation), another A-Train member, can serve the same purpose as CloudSat in deriving CTH. Furthermore, the cloud-profiling capability of the CloudSat 94-GHz CPR identifies the convective part of the system [e.g., *Sassen and Wang*, 2008], excluding stratiform precipitation and anvils. Estimation of $q'_v - q_v$ can be conducted in a similar way since moisture inside clouds is assumed to be saturated so $q'_v$ is only a function of T′. Temperature and moisture contributions can be combined as $g\frac{T'_v - T_v}{T_v}$, where $T_v$ is virtual temperature. The last term - hydrometeor loading - is obtained from CloudSat cloud water content product, but its contribution to convective top buoyancy is found to be at least one order of magnitude smaller than that of the virtual temperature variation unless $|T'_v - T_v| < 0.1$ K (which is too small for satellite instruments to measure anyway). So, we ignore this term in our current study.

[7] Non-black cloud-top IR emissivity is accounted for using collocated CALIPSO lidar. Since the CALIPSO lidar signal cannot penetrate beyond an optical thickness (TAU) of ~3 (Z. Wang and U. Wyoming, private communication, 2010), we have a measure, from CALIPSO, of this depth (which we call $\Delta Z_1$). Using the visible-to-IR conversion [e.g., *Rossow et al.*, 1996], we convert the visible TAU = 3 to the corresponding IR TAU (which we call $TAU_{IR}$). Then, dividing $\Delta Z_1$ by the $TAU_{IR}$ gives an estimation of the depth corresponding to $TAU_{IR} = 1$, which we interpret as the emission level of the IR radiation (referred to as $\Delta Z_2$). Finally, we translate $\Delta Z_2$ into a temperature correction assuming a moist adiabatic lapse rate inside clouds and apply it to correct the IR $T_b$ from the emission level to the height level that corresponds to the CTH by CALIPSO (note that for convective cores, CTH by CloudSat and CALIPSO only differs by ~300 m).

[8] Compared to buoyancy, entrainment of environmental air into convection is less straightforward to characterize. A number of ways have been proposed to model convective entrainment [*Houze*, 1993; *Emanuel*, 1994]. For simplicity, we adopt the entraining plume model approach that is often used in GCM cumulus parameterization [e.g., *Arakawa and Schubert*, 1974; *Lin and Arakawa*, 1997]. According to the entraining plume model, convective entrainment rate ($\lambda$; unit: %/km) is related to vertical changes of moist static energy ($MSE \equiv C_pT + gz + L_vq$, where T, z, and q refer to temperature, height and specific humidity, respectively; $C_p$ is the specific heat of dry air, g gravitational acceleration, and $L_v$ the latent heat of condensation) as: $\frac{\partial MSE_p}{\partial z} = \lambda(MSE_e - MSE_p)$, where subscripts p and e refer to properties of the in-cloud air parcel and of the environment, respectively. For a given $\lambda$, we can integrate this equation for $MSE_p$ from the planetary boundary layer (PBL) to cloud top using collocated ECMWF operational analysis data to represent the ambient environment. $\lambda$ is determined iteratively, starting from 1%/km and increasing by 1%/km each step until the calculated $MSE_p$ at cloud top is approximately equal to the satellite-inferred MSE (i.e., MSE inferred from CTH and CTT, as well as the assumption that relative humidity is 100% near cloud top). The originating $MSE_p$ in the boundary layer is assumed to be the same as that of the environment ($MSE_e$).

[9] It should be noted that convective entrainment and cloud-top buoyancy are closely related. This is actually a unique aspect of our method, that is, unlike previous studies that assume neutral buoyancy for convective plumes [e.g., *Jensen and Del Genio*, 2006; *Kahn et al.*, 2007], we estimate $\lambda$ and B simultaneously. Figure 1 illustrates the connection between $\lambda$ and B using three idealized cases: they are convective plumes of the same height (5 km), the only difference being that one is positively buoyant, one neutrally buoyant, and the other negatively buoyant near cloud top. Viewed in snapshot (as by A-Train), they all appear to be cumulus congestus (Cg). However, their entrainment rates are very different: the positively buoyant Cg has $\lambda$ = 5%/km (least diluted), whereas the negatively buoyant Cg has $\lambda$ = 50%/km (most diluted). Assuming neutral buoyancy, as done in previous studies, will give $\lambda$ = 20%/km. Real examples of these Cg cases are observed from A-Train [*Luo et al.*, 2009]. *Luo et al.* [2009] defined the positively buoyant Cg as "transient" Cg (because they will continue to rise) and the neutrally/negatively buoyant Cg as "terminal" Cg. Some "transient" Cg are likely deep convection in early life stage captured by CloudSat as passing snapshot. Our ongoing study seeks to validate this interpretation using geostationary satellite data with "continuous" temporal coverage.

[10] Data products used in this study and convection selection criteria are almost identical to *Luo et al.* [2009]. Specifically, 2B-GEOPROF data are used for CTH and radar reflectivity, MODIS-AUX for IR $T_b$, and ECMWF-AUX for ambient sounding. *Stephens et al.* [2008] provides an overview of these products and references. The only addition is collocated CALIPSO data, which we obtained from Tohoku University (H. Okamoto, private communication, 2009) and are used for the IR non-black correction. We exclude shallow convection (CTH < 3 km) in this study to avoid unnecessary complication at the early stage of developing the method due to small sizes of the shallow convection. We will consider them in a separate study in the future. To minimize errors due to inhomogeneous cloud tops, we further require that $T_b$ vary by less than 1 K within the $3 \times 3$ grids of 1-km MODIS data centered on each CloudSat profile location. A total of 5939 convective plumes are selected

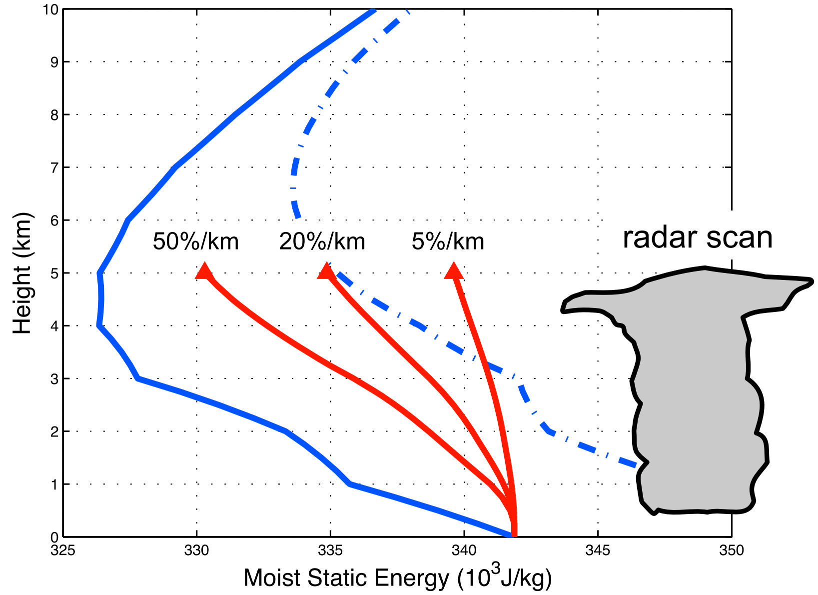


**Figure 1.** Three idealized cases of apparent cumulus congestus in snapshot view shown in red triangles in the diagram of moist static energy. The red curves show the thermodynamic paths of the air parcels rising from the surface layer to the cloud top (5 km). Air Force Geophysics Laboratory reference tropical profile [*Ellingson et al.*, 1991] is used as the ambient sounding.

for the tropics (15S–15N) from September to November 2006.

## 3. Initial Results

[11] Figure 2 shows some initial results in terms of histograms of $\Delta T \equiv T'_v - T_v$ (which is proportional to B) and $\lambda$ as functions of CTH over the tropical oceans. Histograms are normalized at each height level (so they add up to 100% at each level). The rightmost panel shows the histogram of CTH. We briefly summarize the results:

[12] 1. We first note that the convective clouds studied here have two modes: one with CTH at 6–8 km and the other near 12–16 km. They correspond to, respectively, the cumulus congestus (Cg) and deep convective (DC) as described by *Johnson et al.* [1999]. Shallow convection was not included in this study.

[13] 2. Almost all the DC (97%) have negatively buoyant cloud tops. The absolute value of the negative buoyancy increases with CTH. This is consistent with our understanding of moist adiabatic ascent: convective plumes overshooting the corresponding level of neutral buoyancy (~12 km for tropical convective region) become increasingly colder than the environment.

[14] 3. 23% of the Cg (3 km < CTH < 9 km) show positive buoyancy (i.e., "transient" Cg) and 77% show negative buoyancy (i.e., "terminal" Cg). So, if cloud-top buoyancy is not taken into proper account, polar-orbiting satellites will generally overestimate the occurrence frequency of Cg.

[15] 4. In general, DC has smaller entrainment rates: $\lambda$ is concentrated around <10%/km. For Cg, the $\lambda$ distribution seems to be more spread out from <10%/km to 50%/km. Plotting $\lambda$ against B for Cg (not shown) suggests that the larger $\lambda$ values are mostly associated with negative buoyancy ("terminal" Cg) and the smaller $\lambda$ values with positive buoyancy ("transient" Cg). This is consistent with our understanding of the origins of the two types of Cg.

## 4. Uncertainty Analysis and Comparisons With Previous Studies

[16] In this section, we discuss inherent uncertainties associated with the estimated B and $\lambda$. Most of the errors

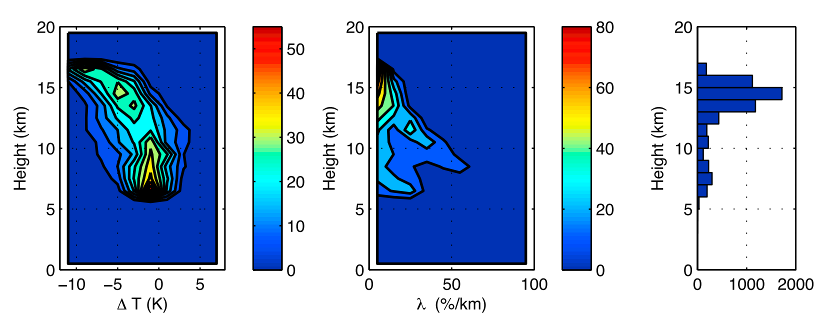


**Figure 2.** Histograms of (left) $\Delta T \equiv T'_v - T_v$ and (middle) entrainment rates as functions of CTH. Histograms are normalized at each height level (so they add up to 100% at each level). Color scale is percentage. (right) Histogram of CTH for the selected convective plumes.

**Table 1.** Sensitivity Tests of the Estimated Entrainment Rates ($\lambda$) for Two Idealized Cases[a]

| | Control | Cloud Top MSE (+3 kJ/kg) | Cloud Top MSE (−3 kJ/kg) | PBL MSE (+3 kJ/kg) | PBL MSE (−3 kJ/kg) | RH (+15%) | RH (−15%) |
|---|---|---|---|---|---|---|---|
| Case 1: DC | 10 | 4 | 21 | 12 | 6 | 12 | 8 |
| Case 2: Cg | 17 | 8 | 31 | 21 | 11 | 24 | 13 |

[a](1) DC with CTH = 10 km and $T' - T = -3$ K (negative buoyancy), and (2) Cg with CTH = 5 km and neutral buoyancy (i.e., $T' - T = 0$ K). The numerical values in the table are the estimated $\lambda$ (unit: %/km).

for B come from temperatures (contribution of moisture variation is insignificant unless $|T' - T| < 0.5$ K, which is considered small compared to temperature errors). The environmental temperature is taken from collocated ECMWF, and in the tropics, ECMWF temperatures are accurate to within 0.5 K as shown by comparison with independent aircraft measurements [*Luo et al.*, 2008c]. Hence, T′ (i.e., CTT) is the major source of uncertainty, which can be further divided into systematic and random errors. IR non-black effect is a systematic error (warm bias), but we made attempt to correct for it using lidar data. Our ongoing research seeks to assess the effectiveness of the correction; without more information at this time, we simply assume a remaining 1–2 K warm bias because dividing $\Delta Z_1$ by $TAU_{IR}$ may underestimate the depth of the IR emission level due to the assumption of constant hydrometer concentration across this depth. Random error in T′ is related to the way $T_b$ is calculated: we estimate $T_b$ by averaging it among the 3 × 3 grids of 1-km MODIS data centered on each CloudSat profile location. To minimize this random error, we require that cloud top is uniform enough so that the standard deviation of the nine $T_b$ readings is within 1 K. An error of 1 K is small for DC because most of them (96%) have $T' - T < -1$ K. For Cg, however, random error of 1 K casts 59% of the "transient" Cg and 31% of the "terminal" Cg into the uncertainty zone, that is, their "transient"/"terminal" status is no longer distinct. A systematic warm bias of 1–2 K in T′, if exists, will result in an increase in "terminal" Cg at the expense of "transient" Cg by similar amounts. It should be noted that, despite the uncertainties in the fraction of "terminal" and "transient" Cg, they do not affect the general conclusion that both types of Cg are present and consequently, all previous estimations of the occurrence frequency of Cg based on polar-orbiting satellites are overestimates.

[17] Uncertainties in entrainment rates can be attributed to the following error sources: 1) CTT and CTH (which collectively determine the cloud-top MSE), 2) ambient sounding, and 3) PBL inhomogeneity (which affects the originating MSE). As an attempt to gain some insights into how these errors are passed to the estimated entrainment rates, we conduct a sensitivity test using two idealized convective cases: one for DC and the other for Cg (specifics of the two cases are given in Table 1). We first estimate the magnitude of the error sources: 1) CTT is assumed to have an error of 1–2 K, following the discussion in the previous paragraph. CTH uncertainty is assumed to be one CloudSat CPR range gate - 240 m. They contribute to the uncertainty of the cloud-top MSE by ~3000 J/kg. 2) Ambient temperature profile is considered accurate but relative humidity (RH) has an error bar of ±15% (relative sense), based on the evaluation of ECMWF humidity data by *Luo et al.* [2008c]. 3) PBL inhomogeneity is difficult to estimate. Without more information, we use ±3000 J/kg perturbations to the originating MSE in the PBL for the sensitivity test, which is probably reasonable for marine boundary layer (note Figure 2 is shown for the tropical oceans). Once these three error sources are specified, we calculate their impacts on the estimated entrainment rates. Air Force Geophysics Laboratory reference tropical profile [*Ellingson et al.*, 1991] is used as the ambient sounding. The sensitivity test results are shown in Table 1. The largest error comes from the cloud-top conditions: uncertainty in cloud-top MSE affects the entrainment rates by −53% to 110% in a relative sense. Errors in ambient profile and PBL inhomogeneity, in contrast, have a lesser impact and affect the entrainment rates by −24% to 41% (relative sense). These sensitivity tests highlight the range of uncertainty that is expected of the results and underscores the importance of accurately measuring CTT and CTH. Further refinement of the method will be made along this direction. To put these seemingly significant error bars in proper context, we note that the difference in $\lambda$ between "transient" and "terminal" Cg as shown in Figure 2 ranges from several hundred percent to an order of magnitude (i.e., from less than 10%/km to 50%/km).

[18] Finally, we briefly compare our results to a few recent studies. *Jensen and Del Genio* [2006] estimated the entrainment rates for 67 cases of Cg observed by the ARM (Atmospheric Radiation Measurement) climate research facility near Nauru Island: most of them range from 10%/km to 50%/km, broadly in agreement with our Cg cases. However, the results of the current study are based on a much larger sample over the whole tropical oceans. In another study by Dieter Kley and the senior author (to be submitted to JGR), four years of ozone and temperature measurements made on board commercial aircraft near deep convective outflow have been analyzed to estimate entrainment rates of deep convection occurring in the tropical Atlantic; their results give a distribution of $\lambda$ from 5%/km to 15%/km with the mode at 11%/km, which, again, broadly agrees with our estimates for the DC cases.

## 5. Summaries and Discussion

[19] This study describes a satellite-based method to estimate simultaneously convective buoyancy (B) and entrainment rate ($\lambda$). We use A-Train data to illustrate the method, but it will apply to future satellite missions such as EarthCare in a similar way. The measurement requirements are cloud-top height (CloudSat/CALIPSO), cloud-top temperature (MODIS), cloud profiling information (CloudSat/CALIPSO), as well as environmental sounding (ECMWF). CALIPSO lidar is also used to correct for the IR non-black effect near cloud top. Initial results for the tropical oceans are presented and discussed in light of our current understanding of tropical convection. It is found that tropical oceanic convection above the PBL fall into two groups: deep convection (DC) and cumulus congestus (Cg). DC tend to have negative buoyancy near cloud top and $\lambda$ is generally

<10%/km. Cg are further divided into two groups due to the snapshot view of A-Train: "transient" Cg have positive buoyancy near cloud top and $\lambda$ values $\leq$ 10%/km, whereas "terminal Cg" have negative buoyancy near cloud top and $\lambda$ reaching up to 50%/km. Uncertainty analysis is conducted showing that estimation in cloud-top temperature and cloud-top height is the primary source of errors, but they do not affect our conclusions qualitatively. Brief comparisons with previous studies indicate the results of this study are broadly consistent with these earlier studies.

[20] Although most of the initial results are expected, it is important to point out that this study represents the first time, to our knowledge, that satellite data are used to simultaneously estimate convective buoyancy and entrainment rate. A number of potential applications can be pursued with this new satellite capability. For example, an ensemble of convective plumes can be collected from A-Train constellation within a certain climate regime or a certain phase of the Madden-Julian Oscillation. With estimated entrainment rates, these satellite observations can be directly compared to GCM cumulus parameterizations, especially those using *Arakawa and Schubert*'s [1974] approach where cumulus ensemble is represented by a spectrum of entraining plumes with characteristic entrainment rates. Other applications may include investigation of environmental control of cumulus congestus, similar to the ground-based study by *Jensen and Del Genio* [2006], but on a global basis. Our ongoing study pursues these routes.

[21] **Acknowledgments.** We thank Hajime Okamoto of Tohoku University for providing collocated CALIPSO data. The study was supported partly by the NASA MAP projects under grants NNX09AJ46G and NNX09AJ45G and partly by CCNY new faculty startup fund. The senior author would like to thank Andy Ackerman, Ann Fridlind, Anthony Del Genio, and William Rossow for insightful discussion during the joint CCNY-GISS convection seminar.

## References

Arakawa, A., and W. H. Schubert (1974), Interaction of a cumulus cloud ensemble with the large-scale environment, Part I, *J. Atmos. Sci.*, *31*, 674–701, doi:10.1175/1520-0469(1974)031<0674:IOACCE>2.0.CO;2.

Ellingson, R. G., J. Ellis, and S. Fels (1991), The intercomparison of radiation codes used in climate models: Longwave results, *J. Geophys. Res.*, *96*, 8929–8953, doi:10.1029/90JD01450.

Emanuel, K. A. (1994), *Atmospheric Convection*, 580 pp., Oxford Univ. Press, New York.

Heymsfield, A. J., P. N. Johnson, and J. E. Dye (1978), Observations of moist adiabatic ascent in northeast Colorado cumulus congestus cloud, *J. Atmos. Sci.*, *35*, 1689–1703, doi:10.1175/1520-0469(1978)035<1689:OOMAAI>2.0.CO;2.

Houze, R. A., Jr. (1993), *Cloud Dynamics*, *Int. Geophys. Ser.*, vol. 53, 573 pp., Academic, San Diego, Calif.

Jensen, M. P., and A. D. Del Genio (2006), Factors limiting convective cloud-top height at the ARM Nauru Island climate research facility, *J. Clim.*, *19*, 2105–2117, doi:10.1175/JCLI3722.1.

Johnson, R. H., T. M. Rickenbach, S. A. Rutledge, P. E. Ciesielski, and W. H. Schubert (1999), Trimodal characteristics of tropical convection, *J. Clim.*, *12*, 2397–2418, doi:10.1175/1520-0442(1999)012<2397:TCOTC>2.0.CO;2.

Kahn, R. A., W.-H. Li, C. Moroney, D. J. Diner, J. V. Martonchik, and E. Fishbein (2007), Aerosol source plume characteristics from space-based multiangle imaging, *J. Geophys. Res.*, *112*, D11205, doi:10.1029/2006JD007647.

Lin, C., and A. Arakawa (1997), The macroscopic entrainment process of simulated cumulus ensemble. Part II: Testing the entraining plume model, *J. Atmos. Sci.*, *54*, 1044–1053, doi:10.1175/1520-0469(1997)054<1044:TMEPOS>2.0.CO;2.

Luo, Z., G. Y. Liu, G. L. Stephens, and R. H. Johnson (2009), Terminal versus transient cumulus congestus: A CloudSat perspective, *Geophys. Res. Lett.*, *36*, L05808, doi:10.1029/2008GL036927.

Luo, Z., G. L. Stephens, K. A. Emanuel, D. G. Vane, N. D. Tourville, and J. M. Haynes (2008a), On the use of CloudSat and MODIS data for estimating hurricane intensity, *IEEE Geosci. Remote Sens. Lett.*, *5*, 13–16, doi:10.1109/LGRS.2007.905341.

Luo, Z., G. Y. Liu, and G. L. Stephens (2008b), CloudSat adding new insight into tropical penetrating convection, *Geophys. Res. Lett.*, *35*, L19819, doi:10.1029/2008GL035330.

Luo, Z., D. Kley, R. H. Johnson, and H. Smit (2008c), Ten years of measurements of tropical upper-tropospheric water vapor by MOZAIC. Part II: Assessing the ECMWF humidity analysis, *J. Clim.*, *21*, 1449–1466, doi:10.1175/2007JCLI1887.1.

Rossow, W. B., W. Walker, D. Beuschel, and M. Roiter (1996), International Satellite Cloud Climatology Project (ISCCP) documentation of new datasets, *WMO Rep. 737*, World Meteorol. Organ., Geneva, Switzerland.

Sassen, K., and Z. Wang (2008), Classifying clouds around the globe with the CloudSat radar: 1-year of results, *Geophys. Res. Lett.*, *35*, L04805, doi:10.1029/2007GL032591.

Stephens, G. L., et al. (2002), The CloudSat mission and the A-Train: A new dimension of space-based observations of clouds and precipitation, *Bull. Am. Meteorol. Soc.*, *83*, 1771–1790, doi:10.1175/BAMS-83-12-1771.

Stephens, G. L., et al. (2008), CloudSat mission: Performance and early science after the first year of operation, *J. Geophys. Res.*, *113*, D00A18, doi:10.1029/2008JD009982.

G. Y. Liu and Z. J. Luo, Department of Earth and Atmospheric Sciences, City College of New York, New York, NY 10031, USA. (luo@sci.ccny.cuny.edu)

G. L. Stephens, Department of Atmospheric Science, Colorado State University, Fort Collins, CO 80523, USA.